Predictive Models of Biohydrogen and Biomethane Production Based on the Compositional and Structural Features of Lignocellulosic Materials

Florian Monlau, Cécilia Sambusiti, Abdellatif Barakat, Xinmei Guo, Eric Latrille, Eric Trably, Jean-Philippe Steyer, Hélène Carrère

Predictive models of biohydrogen and biomethane production based on the compositional and structural features of lignocellulosic materials

Florian MONLAU[1], Cecilia SAMBUSITI[2], Abdellatif BARAKAT[3], Xin Mei GUO[1], Eric LATRILLE[1], Eric TRABLY[1], Jean-Philippe STEYER[1], Hélène CARRERE[1*]

[1]INRA, UR050, Laboratoire de Biotechnologie de l'Environnement, Avenue des Etangs, 11100 Narbonne, France.

[2] Politecnico di Milano, DIIAR, Environmental Section, Piazza L. da Vinci, 32, 20133, Milano, Italy.

[3] INRA, UMR IATE 1208, Ingénierie des Agro polymères et Technologies Emergentes, 2, place Pierre Viala F- 34060 Montpellier, France.

*** phone: +33 4 68 42 51 68, fax +33 4 68 42 51 60; Email: helene.carrere@supagro.inra.fr**

KEYWORDS: lignocellulosic biomass, structural features, anaerobic digestion, dark fermentation, crystallinity

Abstract:

In an integrated biorefinery concept, biological hydrogen and methane production from lignocellulosic substrates appears to be one of the most promising alternatives to produce energy from renewable sources. However lignocellulosic substrates present compositional and structural features that can limit their conversion into biohydrogen and methane. In this study, biohydrogen and methane potentials of twenty lignocellulosic residues were evaluated. Compositional (lignin, cellulose, hemicelluloses, total uronic acids, proteins and soluble sugars) as well as structural features (crystallinity) were determined for each substrate. Two predictive Partial Least Square (PLS) models were built to determine which compositional and structural parameters affected biohydrogen or methane production from lignocellulosic substrates, among proteins, total uronic acids, soluble sugars, crystalline cellulose, amorphous holocelluloses and lignin. Only soluble sugars had a significant positive effect on biohydrogen

production. Besides, methane potentials correlated negatively to the lignin contents. In a lower extent, crystalline cellulose showed also a negative impact on methane potentials. In contrast, soluble sugars, proteins and amorphous hemicelluloses increased the methane production. These findings will help to develop further pretreatment strategies for enhancing both biohydrogen and methane production.

Graphical abstract:

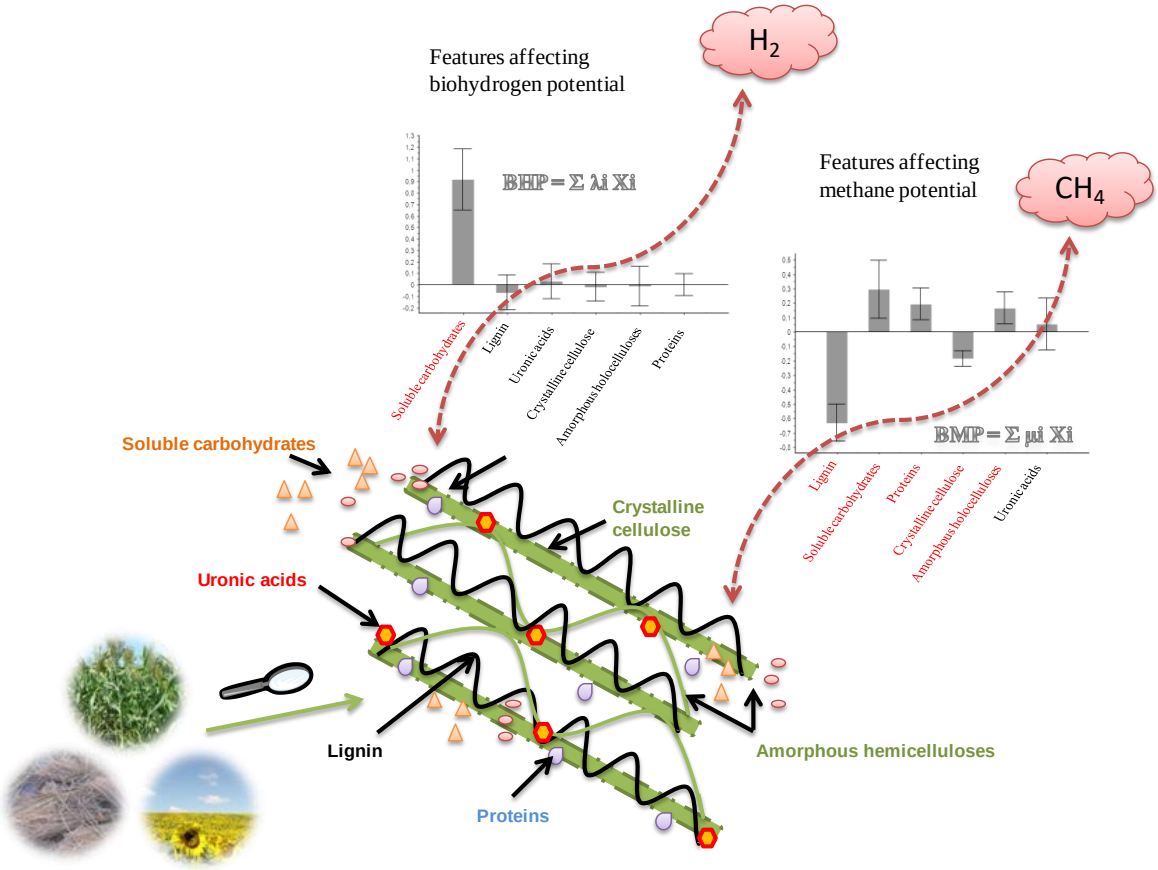

Introduction:

Development of new technologies for renewable energy generation such as biohydrogen and biomethane from lignocellulosic materials in a concept of integrated biorefinery appears as a very promising alternative to fossil fuels [1,2]. Worldwide, the lignocellulosic biomass was evaluated about 200 billion tons annually [3]. The use of lignocellulosic biomass, and more particularly agricultural residues as bioenergy sources is interesting because of (i) its renewability, (ii) it provides additional incomes to farmers, (iii) it uses the non edible part (stalks, leaves) of the plants and thus does not enter in competition with food and (iv) it permits to treat residues which are often burnt in the field creating environmental pollution [3,4].

Methane is produced by a biological process in four steps (hydrolysis, acidogenesis, acetogenesis and methanogenesis) so-called anaerobic digestion. Biohydrogen is produced by dark fermentation which consists of an intermediate stage of anaerobic digestion where the last step of methanogenesis does not occur. Biohydrogen and methane can be produced using undefined mixed microbial cultures [2,5]. Mixed cultures are easier to use than pure cultures as they do not require aseptic conditions and can convert a large range of feedstocks into biohydrogen or methane [6,7]. Nevertheless, in the case of biohydrogen production with mixed cultures, it is necessary to apply heat shock or chemical pretreatments in order to block the conversion of acetate or hydrogen and carbon dioxide into methane [5].

Lignocellulosic substrates are composed of three main fractions: lignin, cellulose and hemicelluloses. Contrary to lignin, the holocelluloses, ie cellulose and hemicelluloses, can be converted into biohydrogen and methane [2]. Nevertheless, lignocellulosic substrates present structural features that limit the accessibility of holocelluloses to microorganisms and thus their conversion to biohydrogen or methane.

Only few studies have attempted to give some insights on the effect of compositional and structural features of lignocellulosic substrates on biohydrogen and methane production [8-12]. The

67 correlations found in the literature between the composition of lignocellulosic residues and
68 biohydrogen or methane production are summarized in Table 1.
69 For hydrogen production, Guo et al., (2012) recently showed a good correlation (R^2 =0.89)
70 between biohydrogen yields and soluble carbohydrates extracted under mild acidic conditions (2
71 N hydrochloric acid) [12]. The main bottleneck of using lignocellulosic biomass in dark
72 fermentation processes is to convert holocelluloses into fermentable sugars [13]. Recently, Yuan et
73 al. (2011) showed that hydrogen production from wheat straw was well correlated with the
74 degradation of cellulose and hemicelluloses into fermentable sugars [14]. However, knowledge
75 about the effect of compositional and structural features on biohydrogen potentials remains very
76 limited.
77 According to Gunaseelan (2007), methane potentials can be predicted from five main chemical
78 constituents (total soluble carbohydrate, acid detergent fibers (ADF), lignin/ADF, nitrogen and
79 ash) which accounted for 90% of the total variation in methane potentials (R^2=0.90) [8]. Negative
80 correlations were also found between lignin contents and biochemical methane potentials for
81 manure and energy crops (R^2=0.88) [11]. Similarly, Buffiere et al. (2006) showed a negative
82 correlation between anaerobic biodegradability and the sum of cellulose and lignin contents [10]. In
83 contrast, Eleazer et al. (1997) reported that methane potentials from several municipal solid
84 wastes correlated positively to the sum of cellulose and hemicelluloses contents [15]. In all these
85 studies, lignin seemed to be the main restrictive factor for methane production, likely by limiting
86 the microbial accessibility to holocelluloses during the fermentative process [2,16]. Overall, the
87 effect of other compositional features, especially cellulose, is still not clear and sometimes
88 contradictory between the different studies.
89 Except models established by Gunasselan (2007 and 2009), all models previously described were
90 built with only one or two compositional characteristics [8,9]. Moreover, only compositional
91 features have been considered and the effect of structural characteristics such as cellulose

crystallinity have not been investigated yet. Indeed, cellulose presents both crystalline and amorphous parts and the crystalline one prevents cell penetration by micro-organisms or extracellular enzymes [17]. Other compositional characteristics such as the presence of pectin (polymer of uronic acids) have not been considered in models. Recently, Pakarinen et al. (2012) showed that pectin removal can significantly increase enzymatic hydrolysis of lignocellulosic substrates [18].

Information about the influence of compositional and structural features on fermentative processes is thus limited especially for biohydrogen production, and sometimes results are contradictory. So the determination of compositional (lignin, holocelluloses, uronic acids and soluble fractions) and structural (crystallinity of cellulose) characteristics appears essential to understand the limitation of lignocellulosic material conversion into biohydrogen or methane. Moreover, this study can be valuable to obtain guidelines for establishing further pretreatment strategies to improve biohydrogen and methane production from lignocellulosic residues.

The objectives of this study were: (1) to characterize the compositional (cellulose, hemicelluloses, lignin, uronic acids, proteins, soluble carbohydrates) and structural features (crystallinity of cellulose) of various lignocellulosic substrates, (2) to evaluate their biohydrogen and methane potentials and (3) to develop multilinear PLS models for predicting biohydrogen and methane potentials from their compositional and structural features.

2. Materials and methods

2.1. Lignocellulosic materials

The substrates used in this study were selected among various lignocellulosic residues, biomass crops and carbohydrate-rich substrates, but no lipid-rich substrate was considered. They corresponded to rice straw, giant reed (stalks and leaves), three varieties of sunflower stalks (1, 2, and 3), sunflower bark, sunflower oil cakes, maize (stalks, leaves and cobs), Jerusalem artichoke (stalks, leaves and tubers), and six varieties of sorghum (1: seed sorghum stalks, 2: biomass sorghum, 4: forage sorghum, 3,5, and 6: sweet sorghum). All substrates were milled into particles of 2 mm using a cutting milling Restch, SM 100. The substrates were analyzed for Total Solids (TS) and Volatile Solids (VS) (Table 1) according to the APHA standard method[19].

2.2. Chemical composition

Soluble sugars (glucose and fructose) from starch, sucrose and inulin were extracted using a mild acid hydrolysis method [20]. Samples (200 mg) were hydrolyzed at 121°C, for 1h, with 0.2% H_2SO_4. The supernatant was filtrated with nylon filters (20 µm) and released carbohydrates (glucose and fructose) were quantified by High-Pressure Liquid Chromatography (HPLC) method coupled to refractometric detection. The analysis was done with a combined Water/Dionex system (Ultimate 3000), using a Biorad HPX-87P column at 85°C. The eluent corresponded to deionized water under a flow rate of 0.6 mL min^{-1}. The system was calibrated with glucose and fructose standards (Sigma–Aldrich®).

Structural-carbohydrates (glucose, xylose, arabinose, uronic acids) from cellulose, hemicelluloses and pectins were measured using a strong acid hydrolysis method adapted from Effland et al. (1977) [21]. Samples (200 mg) were first hydrolyzed with 12 M H_2SO_4 acid for 2 h at room temperature, then diluted to reach a final acid concentration of 1.5 M and kept at 100°C for 3 h. The

insoluble residue was separated from the supernatant by filtration on fibreglass paper (GFF, WHATMAN). This insoluble residue was washed with 50 mL of deionized water and then placed in a crucible. The crucible and the paper fibreglass were dried at 100°C during 24 h to determine by weighing the amount of Klason lignin. The supernatant was further filtrated with nylon filters (20 µm) and analyzed for quantification of monomeric carbohydrates. All monosaccharides (glucose, xylose, arabinose, uronic acids) were analyzed by HPLC coupled to refractometric detection. The analysis was carried out with a combined Water/Dionex system (Ultimate 3000), using a Biorad HPX-87H column at 50°C. The eluent corresponded to 0.005 M H_2SO_4 under a flow rate of 0.3 mL min^{-1}. A refractive index detector (Waters 2414) was used to quantify the carbohydrates. The system was calibrated with glucose, xylose, arabinose, and uronic acids (galacturonic and glucuronic) standards (Sigma–Aldrich®). Thereafter, cellulose and hemicelluloses contents were estimated as follows (equation 1 and 2):

$$\text{Cellulose (\% TS)} = \text{Glucose (\%TS)} / 1.11 \quad (1)$$

$$\text{Hemicelluloses (\% TS)} = [\text{Xylose (\%TS)} + \text{Arabinose (\%TS)}] / 1.13 \quad (2)$$

where 1.11 is the conversion factor for glucose-based polymers (glucose) to monomers and 1.13 is the conversion factor for xylose-based polymers (arabinose and xylose) to monomers according to Petersson et al. (2007) [22].

2.3. Crystallinity measurement assessment

Fourier Transform Infrared Spectroscopy (FTIR) spectroscopy was used to determine the crystallinity of lignocellulosic materials. FTIR spectra were collected in the 4000–600 cm^{-1} range using a Nexus 5700 spectrometer (ThermoElectron Corp.) with built-in diamond ATR single reflection crystal and with a cooled MCT detector. Spectra were recorded in absorption mode at 4 cm^{-1} intervals with 64 scans, at room temperature. Three spectra were recorded for each sample

158 and all spectra pre-treatments were analyzed using Omnic v7.3.software. Among the different
159 FTIR bands, the bands at 1430 and 898 cm^{-1} are sensitive to the amount of crystalline cellulose and
160 amorphous cellulose respectively [23]. The bands ratio H 1430/ H 898 commonly called Lateral Order
161 Indice (LOI) can be used to determine the amount of crystalline cellulose. Using equations 3 and 4,
162 the crystalline cellulose content was estimated (equation 5).
163
164 Cellulose = Crystalline cellulose + Amorphous cellulose (3)
165 LOI = Crystalline cellulose / Amorphous cellulose (4)
166 Crystalline cellulose (IR) = Cellulose x CrI_{IR} (5)
167 Where CrI_{IR} = LOI / (1+LOI)
168 To validate the use of FT-IR spectra to assess cellulose crystallinity, crystallinity was also
169 determined by a more common technology, as X-ray diffraction, on eight lignocellulosic substrates
170 (giant reed stalks, sunflower stalks 1, maize stalks, rice straw, sorghum 1, Jerusalem artichoke
171 stalks, maize cobs and sunflower oil cakes). X-ray measurements were performed in a Philips
172 Analytical X-diffractometer, using Cu Ka radiation at k = 0.1540 nm (40 kV, 40 mA). The
173 measurements were carried out on powder compacted to small mats. DRX data were collected at 2θ
174 angle range from 5° to 50° with a step interval of 0.02°. The degree of crystallinity was expressed
175 as a percentage of crystallinity index (% CrI). The equation used to calculate the CrI was previously
176 described by Segal et al. (1959) in the following form[24]:
177 $CrI_{DRX} = (I_{002}-I_{am})/I_{002})*100$ (6)
178 where I_{002} corresponds to the counter reading at peak intensity at a 2 θ angle of 22° and I_{am} the
179 counter reading at peak intensity at 2θ angle of 16° in cellulose. I_{002} - I_{am} corresponds to the
180 intensity of the crystalline peak and I_{002} is the total intensity after subtraction of the background
181 signal measured without cellulose [25]. Crystalline cellulose was the determined using the equation 7:

182 Crystalline cellulose (DRX) = Cellulose x CrI_{DRX} (7)

183 A good correlation (R^2 = 0.93) was found between crystalline cellulose values determined by DRX
184 and FTIR (Figure 1). However, the amounts of crystalline cellulose determined by FTIR were
185 higher than DRX, likely because CrI_{IR} measurements corresponded only to approximated values.
186 Indeed, although 1430 and 898 cm^{-1} bands are sensitive to the amount of crystalline cellulose and
187 amorphous cellulose, respectively, and each band contains contributions from both crystalline and
188 amorphous regions. Therefore, FTIR measurements must be considered as relative values and the
189 FTIR method was only used to compare crystalline cellulose contents from different lignocellulosic
190 materials.

191

192 **2.4. Biohydrogen and methane production**

193 **2.4.1 BioHydrogen Potential (BHP)**

194 BHP experiments were carried out in batch mode at 37°C. The volume of each flask was 600 mL,
195 with a working volume of 400 mL. A quantity of 3.5 g VS of substrate was initially introduced in
196 each flask. Then, 200 mL of MES (2-[N-morpholino] ethane sulfonic acid, 50 $mmol.L^{-1}$) buffer and
197 3 mL of seed sludge of an anaerobic digester (as inoculum) (final concentration of 225 $mg\text{-}COD.L^{-1}$)
198 were added to the flask. The inoculum was first treated at 90°C for 15 minutes to inhibit the
199 activity of methanogens and enrich in hydrogen producing bacteria. No additional nutrient medium
200 solution was added. The initial pH value was adjusted to 5.5 with NaOH 2 N or 37 % HCl. The
201 headspace of the flasks was flushed with nitrogen gas to reach anaerobic conditions. The
202 experimental procedure ended when the pressure in the flask headspace started to drop off
203 indicating hydrogen consumption. Each experiment was performed in duplicates.

204

205 **2.4.2 Biochemical Methane Potential (BMP)**

206 Lignocellulosic substrates were digested anaerobically in batch anaerobic flasks at 35°C during 40
207 days. The volume of each flask was 600 mL, with a working volume of 400 mL. Each flask
208 contained: macroelements (NH_4Cl, 26 $g.L^{-1}$; KH_2PO_4, 10 $g.L^{-1}$; $MgCl_2$, 6 $g.L^{-1}$; $CaCl_2$, 3 $g.L^{-1}$),
209 oligoelements ($FeCl_2$, 2 $g.L^{-1}$; $CoCl_2$, 0.5 $g.L^{-1}$; $MnCl_2$, 0.1 $g.L^{-1}$; $NiCl_2$, 0.1 $g.L^{-1}$; $ZnCl_2$, 0.05 $g.L^{-1}$;
210 H_3BO_3, 0.05 $g.L^{-1}$; Na_2SeO_3, 0.05 $g.L^{-1}$; $CuCl_2$, 0.04 $g.L^{-1}$; Na_2MoO_4, 0.01 $g.L^{-1}$), bicarbonate
211 buffer ($NaHCO_3$, 50 $g.L^{-1}$), an anaerobic sludge at 5 g $VS.L^{-1}$ and the substrate at 5 g $TS.L^{-1}$. Once
212 the flasks were prepared, a degasification step with nitrogen gas was carried out to obtain anaerobic
213 conditions. The bottles were closed with air impermeable red butyl rubber septum-type stoppers.
214 Bottles were incubated at 35°C and each experiment was carried out in duplicates.

215 **2.4.3 Gas analysis**

216 Biogas volume was monitored continuously with a water displacement method. Acidified water (pH
217 =2) was used to minimize dissolution of carbon dioxide. All volumes were expressed under
218 temperature and pressure standard conditions. The gas composition (O_2, CO_2, CH_4, H_2 and N_2) was
219 analysed using a gas chromatograph (Clarus 580, Perkin Elmer) equipped with two columns, a
220 molecular sieve (Molsieve, 5Å) and a thermal conductivity detector (TCD). One column
221 (RtMolsieve) was used to separate H_2, O_2, N_2 and CH_4, and the second one (RtQBond) was used to
222 separate CO_2 from other gases. The calibration was carried out with a standard gas (Linde ^{TM})
223 composed of 25 % CO_2, 2 % O_2, 10 % N_2 and 5 % H_2 and 58 % CH_4.

224

225 **2.5 Partial least square regression**

226 PLS (Partial Least Square) models were developed using Unscrambler Version 10.2 software
227 (CAMO software, A/S, Oslo, Norway). This method is particularly adapted for data with highly
228 correlated variables. PLS models were used in full cross validation so-called leave-one-out cross
229 validation procedure. This is a model validation method in which one sample is left out iteratively,

a new calibration model is built, and then the sample that was left out is predicted using this model [26]. The iteration is continued until all samples are left once out of the calibration set. The prediction performances of the models were evaluated by calculating the coefficient of determination (R^2) and the root mean square error of the calibration data set (RMSEPc). High R^2 and low RMSEPc values indicate a good predictive robustness of the model. PLS models built were then tested on an independent set, and the root mean square error of independent validation set (RMSEPiv) was calculated to define the quality of the model. The RMSEP was defined as follow:

$$RMSEP = \sqrt{\frac{\sum_1^n (\widehat{yi} - yi)^2}{n}} \quad (8)$$

where: $\widehat{yi}$ is the prediction value of the sample i in a calibration data set (or independent validation set); yi, is the measured BHP or BMP value of the sample i in a calibration data set (or in a independent validation set) and n is the number of samples in calibration data set (or independent validation set).

3. Results and discussion

3.1 Compositional and structural characteristics of the lignocellulosic substrates

Soluble sugars (SolSu), uronic acids (Ua), proteins (Pro), hemicelluloses (Hem), cellulose (Cell), and lignin (Lig) contents of twenty lignocellulosic substrates are presented in Table 2, in % of TS. Soluble sugars (non structural carbohydrates like starch, sucrose and inulin) were mainly present in sorghum substrates (ranging from 8.2 to 22.8 %, except for sorghum 1). Gunaseelan (2007) noticed as well a high content of soluble carbohydrates up to 23 % of VS in sorghum bicolour roots [8]. According to Thuesombat et al. (2007), Jerusalem artichoke presents 70-90% of inulin (linear poly-fructose chain) which explains the high values of soluble sugars found in Jerusalem artichoke stalks and tubers, ie 32.9 % and 59.1 % per TS respectively [27]. Proteins content ranged from 2.3 %

253 (sunflower stalk 2) to 29.7 % (sunflower oil cakes). This result is consistent with Raposo et al.,
254 (2008) who evaluated a protein content of 31 % per TS in sunflower oil cakes [28]. Uronic acids
255 (galacturonic and glucuronic) which originated from both hemicelluloses and pectins were also
256 quantified. Uronic acids contents ranged from 0.2 % (giant reed and Jerusalem artichoke stalks) to 7
257 % (sunflower stalks 1). Concerning the holocelluloses fraction, hemicelluloses content ranged from
258 5 % (Jerusalem artichoke tubers) to 34.6 % (maize cobs) and cellulose contents ranged from 5.4 %
259 (Jerusalem artichoke bulbs) to 33.1 % (giant reed stalks). Crystalline cellulose and amorphous
260 holocelluloses expressed in % TS using FTIR spectra are presented in Table 2. The crystalline
261 cellulose content ranged from 2.5 % for Jerusalem artichoke bulbs to 16.3 % for giant reed stalks.
262 The content of amorphous holocelluloses, which is the sum of amorphous cellulose and
263 hemicelluloses, ranged from 7.5 % (Jerusalem artichoke tubers) to 50.3 % (maize cobs). Finally,
264 lignin content ranged from 12.3 % (Jerusalem artichoke tubers) to 35 % (sunflower stalks bark).
265 Moreover on a same plant, lignin content was found higher in stalks than in leaves, except for giant
266 reeds that presented almost similar lignin contents. Similar trends were observed with 14.1 % and
267 18.4 % of lignin for wheat straw leaves and stalks, respectively [29]. The range of the variables values
268 (% per TS) is relatively high to permit to screen a wide range of compositional and structural
269 features (Table 2).

270

271 3.2 Biological hydrogen potential (BHP) and biological methane potential (BMP) tests

272 Hydrogen and methane potentials of lignocellulosic substrates are presented in Figure 2.
273 Biohydrogen potentials ranged from 1.6 (± 0.1) mL H_2 g^{-1}TS (sunflower stalk bark) to 120 (± 11)
274 mL H_2 g^{-1}TS (Jerusalem artichoke tubers). Similarly to Jerusalem artichoke tubers, Jerusalem
275 artichoke stalks presented an interesting biohydrogen potential as 62 (± 6) mL H_2 g^{-1} TS were
276 produced. Except for sorghum 1, high sorghum hydrogen potentials from 23 (± 1) mL H_2 g^{-1} TS to
277 64 (± 14) mL H_2 g^{-1} TS were observed for sorghum substrates. Similar hydrogen yields were

278 reported on sweet sorghum stalks with 52 mL H_2 g^{-1} VS [30]. Sunflower stalks were found to produce
279 low hydrogen potentials: 1.8 (± 0.9), 2.1 (± 0.7) and 2.5 (± 0.5) mL H_2 g^{-1} TS for sunflower stalks
280 numbers 3, 2, and 1, respectively. With similar lignocellulosic residues, slightly lower hydrogen
281 yields of 1 mL H_2 g^{-1} VS and 3.16 mL H_2 g^{-1} VS were observed for wheat straw and cornstalks,
282 respectively [31,32].

283 In addition, methane potentials ranged from 155 (± 2) mL CH_4 g^{-1} TS (sunflower stalks bark) to 300
284 (± 14) mL CH_4 g^{-1} TS (Jerusalem artichoke tubers). Such results are in agreement with literature
285 data as Dinuccio et al. (2010) found methane potentials of 317 mL CH_4 g^{-1}VS for maize residues,
286 229 mL CH_4 g^{-1}VS for barley straw and 195 mL CH_4 g^{-1} VS for rice straw [33]. Besides Jerusalem
287 artichoke tubers, interesting methane production of 230 (± 18) and 260 (± 4) mL CH_4 g^{-1} TS were
288 observed for Jerusalem artichoke stalks and leaves, respectively. All sorghum substrates present
289 methane potentials higher than 210 (± 33) mL CH_4 g^{-1} TS. Maize leaves and sunflower oil cakes
290 also led to good methane potentials with respectively 235 (± 3) and 244 (± 9) mL CH_4 g^{-1}TS. Low
291 methane potentials were observed for the different varieties of sunflower stalks as 167 (± 27), 172
292 (± 5), and 175 (± 9) mL CH_4 g^{-1}TS for sunflower stalks numbers 3, 1, and 2, respectively.
293 Moreover, on a same plant, the leaves appeared to have higher methane potentials than stalks. As an
294 example, methane potentials of 170 (± 22) and 210 (± 13) mL CH_4 g^{-1} TS were respectively
295 observed for giant reed stalks and leaves, respectively. Overall, all results were lower than 480 mL
296 CH_4 / kg TS which is the theoretical methane potential of lignocellulosic substrates as proposed by
297 Frigon and Guiot (2010) [34]. Some biodegradable parts are indeed not accessible during anaerobic
298 digestion of lignocellulosic substrates likely due to the compositional and structural characteristics
299 that limit the accessibility of microorganisms to holocelluloses, as previously suggested by Triolo et
300 al. (2011) [11].
301
302 3.3 PLS models

One of the main objectives of this study was to identify the compositional and structural features affecting both biohydrogen and methane production from lignocellulosic residues, such as lignin (Lig), amorphous holocelluloses (Am), crystalline cellulose (Cri), protein (Pro), uronic acids (Ua) and soluble sugars (SolSu) contents. PLS models were built on eighteen lignocellulosic substrates and an independent validation set of two substrates (sorghum 1 and sorghum 6) was used to validate the PLS models. Table 2 shows the range values of the variables (Lig, Am, Cri, Pro, Ua, SolSu) in which PLS models are relevant and should not be extrapolated out of these ranges. In particular, the models should not be applied to lipid-rich substrates. Although these models are valid to estimate biohydrogen or methane yields in relation to compositional and structural features of lignocellulosic biomass, they provide no information about substrate degradation rates. Other abiotic and biotic factors such as pH, particle size, accessible surface area, porosity, moisture content,… were not considered and may also impact biohydrogen and methane yields.

3.3.1 Compositional and structural features affecting biohydrogen production

PLS analysis led to equation 9 as a multi-linear model for biohydrogen potentials. The quality of the model to predict hydrogen potential was confirmed by a high R^2 (0.87) and a low value of RMSEPc (11.6 mL H_2 g^{-1} TS).

$$BHP\ (mL\ H_2\ g^{-1}\ TS) = 19.43 + 1.84^*\ SolSu\ (g.g^{-1}\ TS) - 0.36^*\ Lig\ (g.g^{-1}\ TS) + 0.53Ua\ (g.g^{-1}\ TS) - 0.14^*Cri\ (g.g^{-1}\ TS) - 0.05Am\ (g.g^{-1}\ TS) - 0.02^*Pro\ (g.g^{-1}\ TS) \quad (9)$$

This model was validated using a set of two independent samples (sorghum 1 and sorghum 6) which were not included in the calibration data set. Results are presented in Table 3. Hydrogen potentials of 9.2 and 45.9 mL H_2 g^{-1} TS were predicted compared to 9.7 and 37.9 mL H_2 g^{-1} TS measured respectively for sorghum 1 and 6. The REMSEPiv was calculated on the validation data set and a promising result of 5.7 mL H_2 g^{-1} TS was observed showing the high accuracy of the model.

328 Another interest of the PLS models is to determine which variables significantly impact the
329 predicted variable. Centred and reduced weighted regression coefficients for hydrogen potentials
330 are shown in Figure 3a. A strong positive correlation was found between hydrogen potentials and
331 soluble sugars (SolSu) whereas all other studied variables (Lig, Am, Cri, Ua, Pro) had no significant
332 impact. Considering the correlation of hydrogen production versus only soluble carbohydrates, a
333 high correlation of $R^2 = 0.95$ was observed (data not shown). These results are in accordance with
334 Zhang et al., (2007) who suggested that hydrogen yield enhancement was due to an increase of
335 soluble sugar content of the substrate [32]. Recently, Guo et al. (2011) found a similar correlation (R^2
336 = 0.87) between biohydrogen potentials and carbohydrates extracted under mild conditions (2 N
337 hydrochloric acid) [12]. Shi et al. (2012) suggested as well that the enhancement of hydrogen yields
338 nearly coincided with an increase in water soluble sugars available from alkali pretreated and raw
339 sweet sorghum stalks, which were 2.23 and 0.86 g L^{-1}, respectively [30]. Accordingly Pan et al.
340 (2011) showed that hydrolysis of cellulosic biomass led to an enhancement of hydrogen production
341 due to an increase of soluble compounds that were much easier to be degraded [35]. In addition, our
342 results showed that proteins did not affect hydrogen potentials within the range of studied protein
343 contents (< 30% TS – see Table 2). This is consistent with Guo et al. (2012) who reported that hydrogen
344 potentials were lower in the case of protein rich-substrates, but mainly because of their lower contents in
345 carbohydrates[12].

346 In addition, pH is an important factor that can affect biohydrogen production. Although the optimal
347 pH for hydrogen production from carbohydrates is rather acidic (about 4.5 - 6), alkaline pH (about
348 8.5-11) are more favourable for proteins-rich substrates [36,37]. In our study, the initial pH was set up
349 at 5.5 that can explain the absence of significant effect of the protein content. The absence of
350 significant positive correlation between amorphous holocelluloses and hydrogen potentials can be
351 explained by the poor efficiency of H_2-producing bacteria to assimilate directly cellulosic materials.

352 To achieve high yields of hydrogen from lignocellulosic substrates, an hydrolysis step is therefore
353 required [38].
354
355 3.3.2 Compositional and structural features affecting methane production
356 PLS analysis led to equation 10 as a multi-linear model for methane potentials. The quality of the
357 model to predict methane potential was confirmed by a high R^2 (0.88) and a low value of RMSEPc
358 (14.9 mL CH_4 g^{-1} TS).
359 BMP (mL CH_4 g^{-1} TS) = 303.14 – 4.53*Lig ($g.g^{-1}$ TS) + 0.77*SolSu ($g.g^{-1}$ TS) + 1.28*Pro ($g.g^{-1}$
360 TS) -1.59*Cri ($g.g^{-1}$ TS) + 0.61Am ($g.g^{-1}$ TS) +1.33Ua ($g.g^{-1}$ TS) (10)
361 This model was validated using an independent set of two samples (sorghum 1 and sorghum 6)
362 which were not included in the calibration data set. Results are presented in Table 3. Errors of 0.2 %
363 and 4 % between the experimental and predictive methane potentials were observed for sorghum 1
364 and sorghum 6, respectively. The REMSEPiv was calculated on the validation data set, and a result
365 of 6.7 mL CH_4 g^{-1} TS was observed showing the high accuracy of the models. Centred and reduced
366 regression coefficients for the prediction of methane potentials are presented in Figure 3b. In this
367 case, lignin, crystalline cellulose, soluble sugars, amorphous holocelluloses and proteins contents
368 were found to have a significant effect on methane potentials. A strong negative correlation was
369 found between the lignin content and the methane production which is in agreement with other
370 reported studies [11,39-41]. Kobayashi et al. (2004) showed a strong negative correlation (R^2 = 0.95)
371 between the amount of methane produced and the amount of lignin of steam explosed bamboo[41].
372 Triolo et al. (2011) also found a high negative correlation (R^2 = 0.88) between the lignin content
373 and methane potentials of energy crops and manure [11]. However, our results led to a weak
374 correlation (R^2 of 0.82, data not shown) when considering only lignin content and methane

potentials. Consequently, anaerobic biodegradation of lignocellulosic materials into methane is not only related to the lignin content, as suggested elsewhere [11].

PLS regression showed that crystalline cellulose had also a negative impact on methane production but in a lower extent than lignin. Zhu et al. (2009) showed that lignin content and crystallinity are the two dominant parameters affecting negatively the digestibility of lignocellulosic substrates. Moreover, they suggested that cellulose crystallinity could have a higher influence on short time hydrolysis, whereas lignin content could have a higher impact on long time hydrolysis [42].

Additionally, a significant positive correlation was found between methane potentials and the contents in soluble sugars, proteins and amorphous hemicelluloses in our study. According to Hayashi et al. (2005), the readily accessible regions (amorphous regions) of the lignocellulosic biomass are more efficiently hydrolyzed during enzymatic hydrolysis, resulting in the accumulation of crystalline cellulose [43]. Similarly, Scherer et al., (2000) showed that the most degradable part of spent grains corresponded to their soluble and hemicelluloses fractions, while cellulose and lignin were slightly degraded [44]. Besides, giving a quick tool to predict biohydrogen and methane potentials from lignocellulosic substrates, the PLS models built in this study are also valuable to give directions towards the development of pretreatments strategies of lignocellulosic residues for enhancing both biohydrogen and methane production. Pretreatments leading to the solubilisation of hollocelluloses might be recommended for enhancing biohydrogen production whereas delignification, hollocelluloses solubilisation and reducing crystalline cellulose may be recommended for methane production.

Acknowledgements

The authors are grateful to ADEME, the French Environment and Energy Management Agency, for financial support in the form of F. Monlau's PhD grant and to Dr Solhy Abderrahim (INANOTECH Rabat) for his help in DRX analysis.

References

(1) Kaparaju, P.; Serrano, M.; Thomsen, A. B.; Kongjan, P.; Angelidaki, I. Bioethanol, biohydrogen and biogas production from wheat straw in a biorefinery concept. *Bioresource Technol* **2009**, *100*, 2562-2568.

(2) Monlau, F.; Barakat, A.; Trably, E.; Dumas, C.; Steyer, J.-P.; Carrere, H. Lignocellulosic materials into Biohydrogen and Biomethane: impact of structural features and pretreatment. *Crit. Rev. Env. Sci. Tec.* **2012**, *in press,DOI:* 10.1080/10643389.2011.604258.

(3) Ren, N.; Wang, A.; Cao, G.; Xu, J.; Gao, L. Bioconversion of lignocellulosic biomass to hydrogen: Potential and challenges. *Biotechnol. Adv.* **2009**, *27*, 1051-1060.

(4) Sain, M.; Panthapulakkal, S. Bioprocess preparation of wheat straw fibers and their characterization. *Ind. Crop. Prod.* **2006**, *23*, 1-8.

(5) Guo, X. M.; Trably, E.; Latrille, E.; Carrere, H.; Steyer, J. P. Hydrogen production from agricultural waste by dark fermentation: A review. *Int. J. Hydrogen Energ.* **2010**, *35*, 10660-10673.

(6) Li, D. M.; Chen, H. Z. Biological hydrogen production from steam-exploded straw by simultaneous saccharification and fermentation. *Int. J. Hydrogen Energ.* **2007**, *32*, 1742-1748.

(7) Ntaikou, I.; Antonopoulou, G.; Lyberatos, G. Biohydrogen production from biomass and wastes via dark fermentation: a review. *Waste and Biomass Valorization* 2010, *1*, 21-39.

(8) Gunaseelan, V. N. Regression models of ultimate methane yields of fruits and vegetable solid wastes, sorghum and napiergrass on chemical composition. *Bioresource Technol* **2007**, *98*, 1270-1277.

(9) Gunaseelan, V. N. Predicting ultimate methane yields of Jatropha curcus and Morus indica from their chemical composition. *Bioresource Technol* **2009**, *100*, 3426-3429.

(10) Buffiere, P.; Loisel, D.; Bernet, N.; Delgenes, J. P. Towards new indicators for the prediction of solid waste anaerobic digestion properties. *Water Sci. Technol.* **2006**, *53*, 233-241.

(11) Triolo, J. M.; Sommer, S. G.; Moller, H. B.; Weisbjerg, M. R.; Jiang, X. Y. A new algorithm to characterize biodegradability of biomass during anaerobic digestion: Influence of lignin concentration on methane production potential. *Bioresource Technol* **2011**, *102*, 9395-9402.

(12) Guo, X. M.. Biohydrogen production and metabolic patways in dark fermentation related to the composition of organic solid waste. *PhD Thesis, University of Montpellier 2,* **2012**.

(13) Cheng, C. L.; Lo, Y. C.; Lee, K. S.; Lee, D. J.; Lin, C. Y.; Chang, J. S. Biohydrogen production from lignocellulosic feedstock. *Bioresource Technol* **2011**, *102*, 8514-8523.

(14) Yuan, X. Z.; Shi, X. S.; Zhang, P. D.; Wei, Y. L.; Guo, R. B.; Wang, L. S. Anaerobic biohydrogen production from wheat stalk by mixed microflora: Kinetic model and particle size influence. *Bioresource Technol* **2011**, *102*, 9007-9012.

(15) Eleazer, W. E.; Odle, W. S.; Wang, Y. S.; Barlaz, M. A. Biodegradability of municipal solid waste components in laboratory-scale landfills. *Environ. Sci. Technol.* **1997**, *31*, 911-917.

(16) Klimiuk, E.; Pokój, T.; Budzynski, W.; Dubis, B. Theoretical and observed biogas production from plant biomass of different fibre contents. *Bioresource Technol* **2010**, *101*, 9527-9535.

(17) Fan, L.-T.; Lee, Y.-H.; Gharpuray, M. M. The nature of lignocellulosics and their pretreatments for enzymatic hydrolysis. *Adv. Biochem. Eng.* **1982**, *23*, 156-187.

(18) Pakarinen, A.; Zhang, J.; Brock, T.; Maijala, P.; Viikari, L. Enzymatic accessibility of fiber hemp is enhanced by enzymatic or chemical removal of pectin. *Bioresource Technol* **2012**, *107*, 275-281.

(19) (APHA), A. P. H. A. Standard Methods for the Examination of Water and Wastewater, 20th ed. **1998**.

(20) Nguyen S.; Sophonputtanaphoca, S.; Kim, E.; Penner, M.Hydrolytic methods for the quantification of fructose equivalents in herbaceous biomass. *Appl. Biochem. Biotechnol.* **2009**, *158*, 352-361.

(21) Effland, M. J. Modified Procedure to Determine Acid-Insoluble Lignin in Wood and Pulp. *Tappi* **1977**, *60*, 143-144.

(22) Petersson, A.; Thomsen, M. H.; Hauggaard-Nielsen, H.; Thomsen, A. B. Potential bioethanol and biogas production using lignocellulosic biomass from winter rye, oilseed rape and faba bean. *Biomass Bioenerg.* **2007**, *31*, 812-819.

(23) Spiridon, I.; Teaca, C. A.; Bodirlau, R. Structural Changes Evidenced by Ftir Spectroscopy in Cellulosic Materials after Pre-Treatment with Ionic Liquid and Enzymatic Hydrolysis. *BioResources* **2010**, *6*, 400-413.

(24) Segal, L.; Creely, J. J.; Martin Jr, A. E.; Conrad, C. M. An Empirical Method for Estimating the Degree of Crystallinity of Native Cellulose Using the X-Ray Diffractometer. *Textile Res. J.* **1959**, *29*, 786-794.

(25) Park, S.; Baker, J. O.; Himmel, M. E.; Parilla, P. A.; Johnson, D. K. Cellulose crystallinity index: measurement techniques and their impact on interpreting cellulase performance. *Biotechnol. Biofuels* **2010**, *3*, *10*.

(26) Raju, C. S.; Lokke, M. M.; Sutaryo, S.; Ward, A. J.; Moller, H. B. NIR Monitoring of Ammonia in Anaerobic Digesters Using a Diffuse Reflectance Probe. *Sensors* **2012**, *12*, 2340-2350.

(27) Thuesombat, P.; Thanonkeo, P.; Laopaiboon, L.; Laopaiboon, P.; Yunchalard, S.; Kaewkannetra, P.; Thanonkeo, S. The batch ethanol fermentation of jerusalem artichoke using saccharomyces cerevisiae. *Sci. Tech. J.* **2007**, *7*.

(28) Raposo, F.; Borja, R.; Rincon, B.; Jimenez, A. M. Assessment of process control parameters in the biochemical methane potential of sunflower oil cake. *Biomass Bioenerg.* **2008**, *32*, 1235-1244.

(29) Fukushima, R. S.; Hatfield, R. D. Comparison of the Acetyl Bromide Spectrophotometric Method with Other Analytical Lignin Methods for Determining Lignin Concentration in Forage Samples. *J. Agr. Food Chem.*, **2004**, *52*, 3713-3720.

(30) Shi, X. X.; Song, H. C.; Wang, C. R.; Tang, R. S.; Huang, Z. X.; Gao, T. R.; Xie, J. Enhanced bio-hydrogen production from sweet sorghum stalk with alkalization pretreatment by mixed anaerobic cultures. *Int. J. Energy Res.* **2010**, *34*, 662-672.

(31) Fan, Y. T.; Zhang, Y. H.; Zhang, S. F.; Hou, H. W.; Ren, B. Z. Efficient conversion of wheat straw wastes into biohydrogen gas by cow dung compost. *Bioresource Technol* **2005**, *97*, 500-505.

(32) Zhang, M. L.; Fan, Y. T.; Xing, Y.; Pan, C. M.; Zhang, G. S.; Lay, J. J. Enhanced biohydrogen production from cornstalk wastes with acidification pretreatment by mixed anaerobic cultures. *Biomass Bioenerg.* **2007**, *31*, 250-254.

(33) Dinuccio, E.; Balsari, P.; Gioelli, F.; Menardo, S. Evaluation of the biogas productivity potential of some Italian agro-industrial biomasses. *Bioresource Technol* **2010**, *101*, 3780-3783.

(34) Frigon, J. C.; Guiot, S. R. Biomethane production from starch and lignocellulosic crops: a comparative review. *Biofuels Bioprod. Bior.* **2010**, *4*, 447-458.

(35) Pan, C. M.; Ma, H. C.; Fan, Y. T.; Hou, H. W. Bioaugmented cellulosic hydrogen production from cornstalk by integrating dilute acid-enzyme hydrolysis and dark fermentation. *Int. J. Hydrogen Energ.* **2011**, *36*, 4852-4862.

(36) Cai, M. L.; Liu, J. X.; Wei, Y. S. Enhanced biohydrogen production from sewage sludge with alkaline pretreatment. *Environ. Sci. Technol.* **2004**, *38*, 3195-3202.

(37) Xiao, B. Y.; Han, Y. P.; Liu, J. X. Evaluation of biohydrogen production from glucose and protein at neutral initial pH. *Int. J. Hydrogen Energ.* **2010**, *35*, 6152-6160.

(38) Saratale, G. D.; Chen, S. D.; Lo, Y. C.; Saratale, R. G.; Chang, J. S. Outlook of biohydrogen production from lignocellulosic feedstock using dark fermentation - a review. *J. Sci. Ind. Res.* **2008**, *67*, 962-979.

(39) Chandler, J. A.; Jewell, W. J.; Gossett, J.M.; Van Soest, P.J.; Robertson, J.B. Predicting methane fermentation biodegradability. *Biotechnol. Bioeng. Symp.* **1980**, 93-107.

(40) Monlau, F.; Barakat, A.; Steyer, J. P.; Carrère, H. Comparison of seven types of thermo-chemical pretreatments on the structural features and anaerobic digestion of sunflower stalks. *Bioresource Technol* **2012**, *120*, 241-247.

(41) Kobayashi, F.; Take, H.; Asada, C.; Nakamura, Y. Methane production from steam-exploded bamboo. *J. Biosci. Bioeng.* **2004**, *97*, 426-428.

(42) Zhu, L.; O'Dwyer, J. P.; Chang, V. S.; Granda, C. B.; Holtzapple, M. T. Multiple linear regression model for predicting biomass digestibility from structural features. *Bioresource Technol.* **2010**, *101*, 4971-4979.

(43) Hayashi, N.; Kondo, T.; Ishihara, M. Enzymatically produced nano-ordered short elements containing cellulose I[beta] crystalline domains. *Carbohydr. Polym.* **2005**, *61*, 191-197.

(44) Scherer, P. A.; Vollmer, G. R.; Fakhouri, T.; Martensen, S. Development of a methanogenic process to degrade exhaustively the organic fraction of municipal "grey waste" under thermophilic and hyperthermophilic conditions. *Water Sci. Technol.* **2000**, *41*, 83-91.

Captions tables and figures

Table 1: Correlations found in the literature between the compositional characteristics of lignocellulosic substrates and biohydrogen or methane production

Table 2: Compositional and structural features of lignocellulosic substrates and validity range of PLS models. Values correspond to the means of two replicates of independent values ± standard deviations (error bars).

Table 3: External validation of the PLS models for biohydrogen and methane potentials

Figure 1: Correlation between crystalline celluloses determined by IR and DRX (expressed in % TS)

Figure 2: Biochemical biohydrogen and methane potentials of lignocellulosic substrates. Values correspond to the means of two replicates of independent values ± standard deviations (error bars).

Figure 3: Centred and reduced regression coefficients with their 95% confidence intervals for the prediction of biohydrogen potentials (a) and methane potentials (b).

528

529

530 Table 1: Correlations found in the literature between the compositional characteristics of lignocellulosic substrates and biohydrogen or
531 methane production

Fermentation process	Biomass used	Compositional features	Equation	References
Biohydrogen	organic solid substrates (n=21)	Soluble Carbohydrates (Carb)	BHP (mL H_2 . g^{-1} TS) = 1.31 + 199.46 Carb	12
Methane	Manure (n=10), Energy crops (n=10)	Lignin (Lig)	BMP (L CH_4 . kg^{-1} VS) = -1.67*Lig + 421.7	11
Methane	Raw and thermo-chemically pretreated sunflower stalks (n= 8)	Lignin (Lig)	BMP (L CH_4 . kg^{-1} VS) = -0.65*Lig + 379.8	40
Methane	Lignocellulosic residues (n=7)	Soluble carbohydrates (Carb), acid detergent fiber (ADF), Protein (Pro), Lignin (Lig), Ash (A)	BMP (L CH_4 . kg^{-1} VS) = 0.18 + 0.48 *CaRB + 0.2 * ADF -0.003 * Lig/ADF + 2.8 Pro - 0.83 *A	8
Methane	Lignocellulosic residues (n=12)	Soluble carbohydrates (Carb), acid detergent fiber (ADF), Protein (N), Ash (A), Lipids (F)	BMP (L CH_4 . kg^{-1} VS) = 0.045 + 1.23* Carb + 0.24 * Pro + 1.51* F -0.68 * ADF -0.81* Cell - 6.1*A	9
Methane	Lignocellulosic residues (n=15)	Lignin (Lig)	Biodegradability (%MV) = 0.83-1.82*Lig	39
Methane	Municipal solid waste (n=2), agricultural residues (n=2), manure (n=4), vegetables (n=6)	Lignin (Lig), cellulose (Cell)	Biodegradability (%DCO) = 0.87-1.03 (% lignin +% cellulose)	10

Table 2: Compositional and structural features of lignocellulosic substrates and validity range of PLS models. Values correspond to the means of two replicates of independent values ± standard deviations (error bars).

		Chemical composition (% TS)							FT-IR spectra	
Substrates	% TS	SolSu	Pro	Ua	Hem	Cell	Lig	LOI	Cri (% TS)	Am (% TS)
Rice straw	0.96	0.8	5.3 (± 0.2)	0.6 (± 0.1)	18.8 (± 0.7)	26.2 (± 0.5)	27 (± 2.6)	0.85	12	33
Giant reed stalks	0.99	0.3	4.3 (± 0.7)	0.2 (± 0.0)	18.5 (± 0.7)	33.1 (± 1.3)	24.5 (± 0.1)	1.03	16.8	34.8
Giant reed leaves	0.99	2.9	8 (± 0.1)	0.7 (± 0.1)	8 (± 0.1)	20.9 (± 0.6)	25.4 (± 0.1)	0.95	10.2	28.4
Sunflower stalks 1	0.94	0	4.8 (± 0.1)	7.0 (± 0.6)	15.6 (± 0.3)	31 (± 1.6)	29.2 (± 1.6)	1.22	17	29.6
Sunflower stalks 2	0.96	0	2.3 (± 0.4)	3.9 (± 0.4)	14.3 (± 2.4)	31.2 (± 3.1)	27.7 (± 0.2)	1.2	17	28.4
Sunflower stalks 3	0.96	0	4.3 (± 0.7)	2.4 (± 0.2)	14.3 (± 0.7)	31.2 (± 0.7)	30 (± 1.7)	1.18	16.9	28.6
Sunflower stalks bark	0.97	0	2.8 (± 0.4)	1.7 (± 0.3)	13.5 (± 0.2)	27.4 (± 0.4)	35 (± 0.4)	1.1	14.4	26.5
Sunflower oil cakes	0.94	5.2	29.7 (± 3.4)	1.4 (± 0.2)	8.2 (± 0.2)	5.1 (± 0.3)	22.3 (± 2.8)	0.96	3.8	12.1
Maize stalks	0.99	0.4	7.4 (± 0.1)	0.7 (± 0.1)	21.2 (± 0.6)	27.1 (± 0.9)	23.2 (± 0.1)	1.14	14.5	33.9
Maize leaves	0.99	0.3	6.7 (± 0.6)	1.0 (± 0.2)	28.6 (± 3.3)	30.9 (± 3.1)	20.4 (± 0.6)	1.03	15.7	43.8
Maize cobs	0.96	0.2	4.3 (± 0.3)	0.7 (± 0.1)	34.6 (± 1.4)	29.8 (± 1.2)	19.2 (± 1.0)	0.89	14	50.3
Jerusalem artichoke stalks	0.96	32.9	2.8 (± 0.3)	0.2 (± 0.0)	8.8 (± 3.1)	9.6 (± 3.1)	20.3 (± 0.0)	0.95	4.7	13.7
Jerusalem artichoke leaves	0.94	2.6	12.4 (± 0.3)	0.7 (± 0.1)	4.7 (± 0.6)	8.8 (± 1.4)	12.9 (± 1.3)	1.22	4.8	8.6
Jerusalem artichoke tubers	0.98	59.1	10.4 (± 0.2)	1.5 (± 0.2)	5 (± 0.0)	5.4 (± 0.3)	12.3 (± 0.1)	1.1	2.8	7.5
Sorghum 1	0.95	0.4	4.6 (± 0.1)	0.9 (± 0.1)	26.1 (± 0.1)	29.1 (± 0.3)	22.5 (± 1.6)	1.09	15.2	40
Sorghum 2	0.91	15.4	6.5 (± 0.0)	0.6 (± 0.1)	19.4 (± 1.3)	22.2 (± 1.5)	21.4 (± 0.3)	1.05	11.4	28.3
Sorghum 3	0.91	18.5	8.1 (± 0.0)	1.0 (± 0.0)	20.9 (± 1.6)	20.1 (± 1.7)	18.5 (± 0.9)	0.98	10.3	27.9
Sorghum 4	0.94	8.2	8.2 (± 0.0)	0.6 (± 0.0)	21.7 (± 0.2)	18.3 (± 5.8)	20.7 (± 3.0)	1.03	9.3	27.7
Sorghum 5	0.92	22.8	6.9 (± 0.0)	0.6 (± 0.0)	20 (± 1.2)	19.7 (± 0.2)	19.8 (± 1.3)	1.11	10.4	26.2
Sorghum 6	0.88	21.3	6.2 (± 0.0)	0.6 (± 0.0)	18.5 (± 0.8)	18.1 (± 0.1)	21.3 (± 0.0)	1.1	9.5	24.4
Validity range		*0-59.1*	*2.3-29.7*	*0.2-7*	*4.7-34.6*	*5.4-33.1*	*12.3-35*		*2.5-16.3*	*7.5-50.3*

Table 3: External validation of the PLS models for biohydrogen and methane potentials

	PLS model for biohydrogen potentials				PLS model for methane potentials			
Independent samples	BHP measured mL H_2 .g^{-1} TS	BHP predicted mL H_2 .g^{-1} TS	Errors	RMSEPiv	BMP measured mL CH_4 .g^{-1} TS	BMP predicted mL CH_4 .g^{-1} TS	Errors	RMSEPiv
Sorghum 1	9.7	9.2	4.5%	5.7	209.5	209	0.2%	6.7
Sorghum 6	37.9	45.9	21.1%		240	230.5	4.0%	

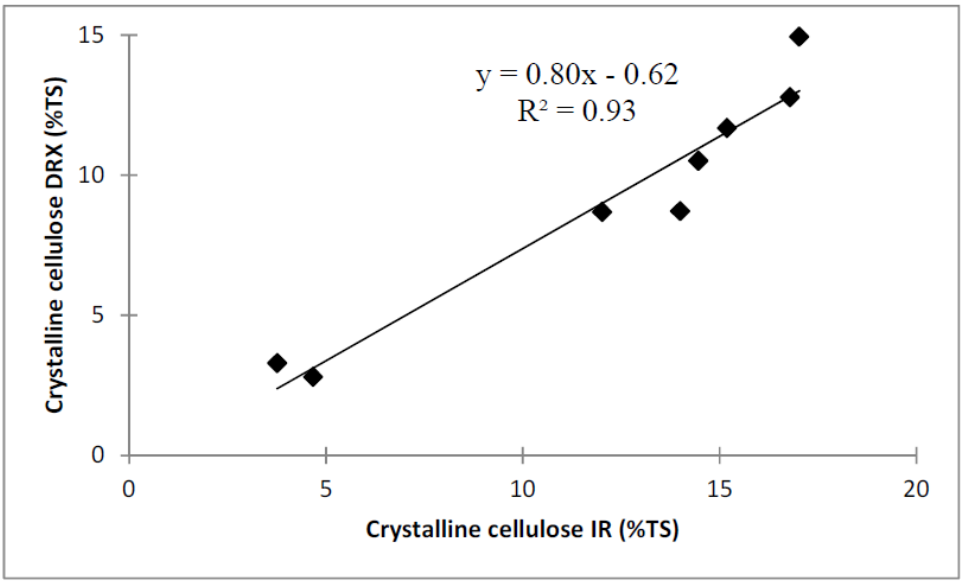

Figure 1: Correlation between crystalline celluloses determined by IR and DRX (expressed in % TS)

545

546

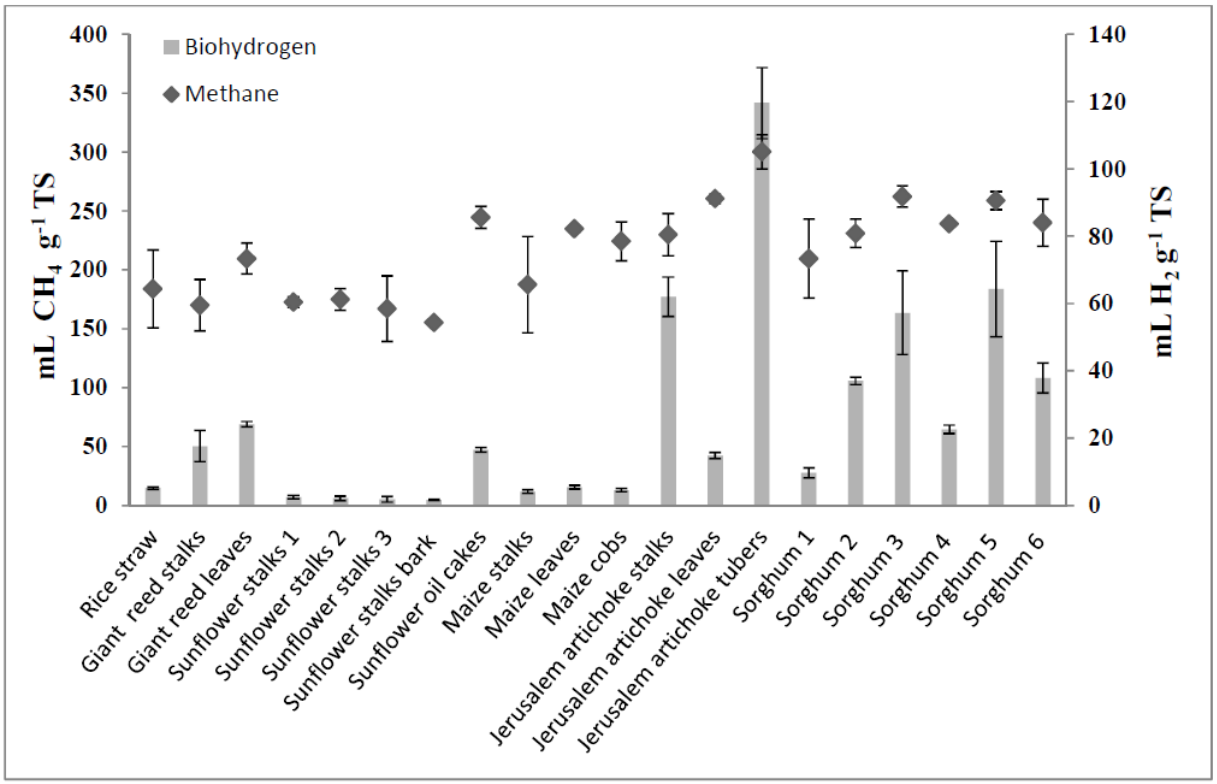

Figure 2: Biochemical biohydrogen and methane potentials of lignocellulosic substrates. Values correspond to the means of two replicates of independent values ± standard deviations (error bars).

547

548

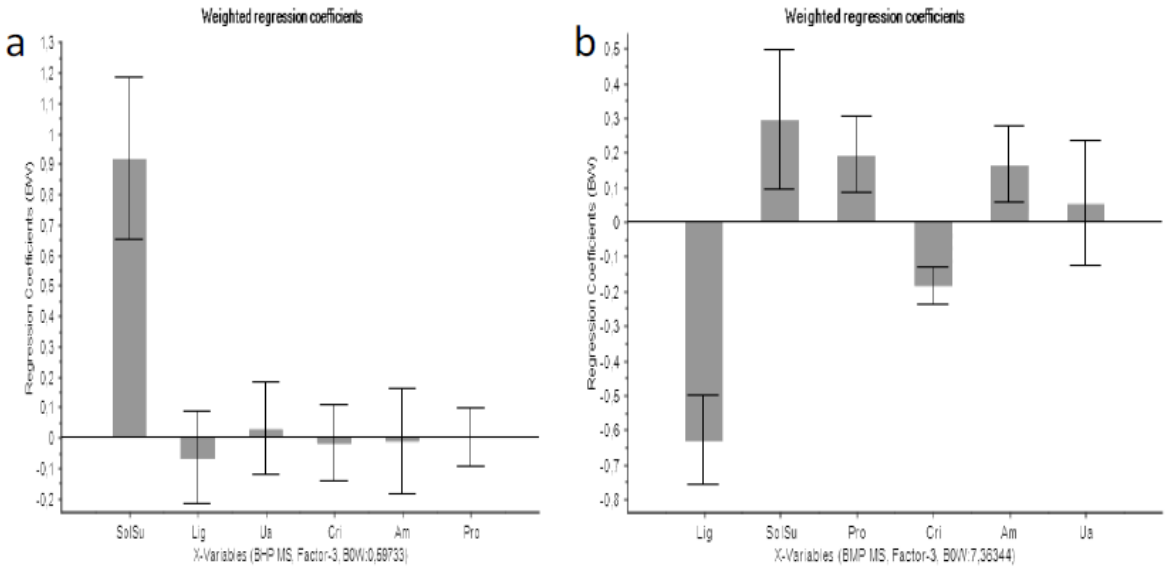

Figure 3: Centred and reduced regression coefficients with their 95% confidence intervals for the prediction of biohydrogen potentials (a) and methane potentials (b).

SolSu= soluble carbohydrates, Lig=lignin Ua= uronic acids, Cri= Crystalline cellulose, Am= amorphous holocelluloses, Pro=proteins

549

550

551